Microplasma Processed Ultrathin Boron Nitride Nanosheets for Polymer Nanocomposites with Enhanced Thermal Transport Performance

ACS APPLIED MATERIALS & INTERFACES

Research Article

www.acsami.org

Microplasma Processed Ultrathin Boron Nitride Nanosheets for Polymer Nanocomposites with Enhanced Thermal Transport Performance

Ri-Chao Zhang,[*,†,‡,§] Dan Sun,[*,‡] Ai Lu,[∥] Sadegh Askari,[⊥] Manuel Macias-Montero,[§] Paul Joseph,[#] Dorian Dixon,[§] Kostya Ostrikov,[¶,▲] Paul Maguire,[§] and Davide Mariotti[§]

[†]Department of Chemical and Biological Engineering, Zhejiang University, Hangzhou, 310002, PR China

[‡]School of Mechanical and Aerospace Engineering, Queen's University Belfast, BT9 5AH, U.K.

[§]Nanotechnology and Integrated Bioengineering Centre (NIBEC), University of Ulster, Newtownabbey, BT37 0QB, Northern Ireland, U.K.

[∥]Institute of Chemical Materials, China Academy of Engineering Physics, Mianyang 621900, Sichuan People's Republic of China

[⊥]Department of Physics, Chemistry and Biology (IFM)/Plasma and Coatings Physics (PLASM), Linköping University, 581 83 Linköping, Sweden

[#]Centre for Environmental Safety and Risk Engineering (CESARE), College of Engineering and Science, Victoria University, Room 4206, Level 2, Building 4 Hoppers Lane, Werribee Campus Victoria 3030, Melbourne, Australia

[¶]School of Chemistry, Physics, and Mechanical Engineering, Queensland University of Technology, Brisbane, Queensland 4000, Australia

[▲]Joint CSIRO−QUT Sustainable Materials and Devices Laboratory, CSIRO, P.O. Box 218, Lindfield, New South Wales 2070, Australia

ABSTRACT: This Research Article reports on the enhancement of the thermal transport properties of nanocomposite materials containing hexagonal boron nitride in poly(vinyl alcohol) through room-temperature atmospheric pressure direct-current microplasma processing. Results show that the microplasma treatment leads to exfoliation of the hexagonal boron nitride in isopropyl alcohol, reducing the number of stacks from >30 to a few or single layers. The thermal diffusivity of the resulting nanocomposites reaches 8.5 $mm^2 s^{-1}$, 50 times greater than blank poly(vinyl alcohol) and twice that of nanocomposites containing nonplasma treated boron nitride nanosheets. From TEM analysis, we observe much less aggregation of the nanosheets after plasma processing along with indications of an amorphous carbon interfacial layer, which may contribute to stable dispersion of boron nitride nanosheets in the resulting plasma treated colloids.

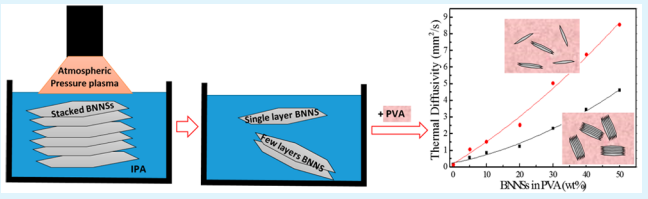

KEYWORDS: *boron nitride, microplasma, thermal transport, exfoliation, phonon, polymer nanocomposites*

INTRODUCTION

Polymer-matrix-based nanocomposite materials is an emerging area in nanotechnology with significant potential for advanced materials design and development. The incorporation and integration of tailored nanoscale filler materials into a polymer matrix can significantly enhance the functionality and performance of the polymer. However, one of the greatest stumbling blocks to the large-scale production and commercialization of nanocomposites is the lack of cost-effective methods for controlling the dispersion of the nanoparticles in polymeric hosts. One common strategy to achieve nanoparticle (NP) colloidal stability is via the chemical binding of ligands to the surface of the nanoparticles, however, a covalent linkage between the ligand and the nanoparticle may alter the properties of the nanoparticles through a modification of their electronic density and the dielectric constant of the surrounding medium[1] and the presence of surfactant/ligand at the organic−inorganic interface often limits the material performance, especially in electrical applications.[2] The other challenge yet to be fully addressed is the weak interfacial interaction between the inorganic and organic phases because of the lack of strong (i.e., covalent) bond between the components. Most dispersion methods still produce composites where the polymer matrix and the fillers interact through relatively weak dispersive forces.[3] Other concerns also remain with the preparation of NPs, such as contamination (from surfactants), the multiple synthesis/processing and purification/cleansing steps required.[4,5]

Received: February 4, 2016
Accepted: May 6, 2016
Published: May 6, 2016

DOI: 10.1021/acsami.6b01531
ACS Appl. Mater. Interfaces 2016, 8, 13567−13572

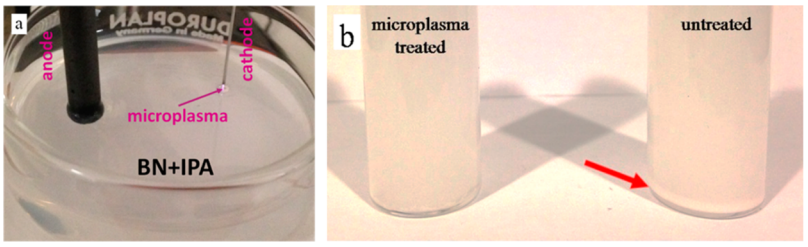

Figure 1. (a) Microplasma setup for h-BN processing. (b) Colloid of h-BN in isopropanol alcohol (IPA) with and without microplasma processing. Red arrow shows the BNNS precipitates which appeared only in untreated samples after 24 h.

Recently, there has been increasing interest in the deployment of two-dimensional (2D) materials, such as graphene and boron nitride (BN) as reinforcement materials in polymer matrix to achieve enhanced functionality of composites. The major difference between BN and graphene is that BN is highly electrically insulating. The excellent mechanical properties, high thermal conductivity and electrical resistivity make BN nanostructures promising additives for creating highly thermally conductive and electrically insulating polymer composites with excellent overall performance suitable for thermal management applications.[6] The exotic properties and high specific surface areas of BN are also important for sensing,[7] catalysis,[8,9] environmental (e.g., water purification)[10,11] and biomedical (e.g., drug delivery)[12] applications.

While BN nanotubes are only available in gram scales and are extremely expensive, BN nanosheets (BNNSs) can be produced in relatively large quantity from hexagonal BN (h-BN) powders. Despite the theoretical thermal conductivity of h-BNNS is on the same order of magnitude as that of graphene (i.e., 1700−2000 W/(mK)),[13−15] the thermal conductivity of BNNS polymer composites has rarely been comparable to those with graphene nanofillers.[6,16−18] h-BN presents highly polar B−N bonds leading to very strong interlayer forces.[19] For this reason, BN sheets are generally found in multilayer stacks, which are difficult to exfoliate to form single or few-layer BNNSs, hence limiting their thermal conduction efficiency.[19−21] Unlike carbon nanostructures, the available chemical reactions to achieve effective surface modifications are very limited for BN nanostructures. The properties of the interface and difficulty in achieving homogeneous dispersion create extensive complications in fabrication of BNNS polymer composites. The above-mentioned facts prevent BNNSs from fulfilling their potential and lead to the properties/functionality of existing BN nanocomposites far from theoretically predicted.

Although exfoliation deploying mechanical milling[22] or using molten hydroxide[23] is possible, the challenge of producing high yield single/few layer BNNSs with controlled quality still remain challenges. In addition, these methods are mostly complicated and time-consuming and often require high temperature or harsh chemicals to be effective, hence may cause contamination or present potential hazard to the environment. Recently, Coleman[24] reported liquid exfoliation through careful selection of suitable solvent to minimize the exfoliation energy. By optimizing the balance of solvent−solvent, solvent−solute and solute−solute binding energies, a 50% yield of single and few-few BNNS (for 0.06 mg/mL BN concentration in IPA) have been achieved.[24]

Recently, some authors of the present paper have shown that plasma-liquid interaction leads to either to direct dispersion of preloaded inorganic nanoparticles (TiO_2) in a polymer solution[25] or the engineering of the surface chemistry of metal NPs to enhance their bond formation with different polymers.[26−28] The improved performance of the resulting composites is a direct result of stable nanoparticle colloidal dispersion and enhanced polymer-NP binding throughout the material, without the use of any additional surfactant or ligand chemistry. This has been achieved by exposing organic polymer and NPs together to high doses of short-lived solvated electrons, reactive radicals and free charge, at low temperature, leading to electrostatic stabilization of the colloid and/or appropriate NP−polymer interfacial chemistries, unhindered by surfactant and ligands.

In this work a room-temperature atmospheric pressure direct-current (DC) microplasmahas been deployed to process h-BN powder in an organic solvent to produce single and few-layers BNNS. Briefly, a microplasma is ignited and sustained at atmospheric pressure above the surface of a colloid mixuture consisting of h-BN dispersed in isopropyl alcohol (IPA). The plasma induced gas/liquid nonequilibrium chemistry results in highly energetic reative species in the liquid phase, which facilitates the depolarization of B−N polar bond and introduces surface modification to the h-BN. Such process has resulted in enhanced exfoliation and dispersion of BNNSs, which when formed a nanocomposite with poly(vinyl alcohol) (PVA), exhibited superior thermal conduction properties.

This is the first report where microplasma processing was deployed to address the issue of 2D nanostructure exfoliation and dispersion. The results demonstrate that microplasma processed BNNSs holds promise for enhanced polymer nanocomposites functionality.

RESULTS AND DISCUSSION

The h-BN/IPA mixture was sonicated for 24 h. The resultant colloid was centrifuged and the supernatant was divided into two samples (plasma treated and untreated). Figure 1a shows an ongoing microplasma treatment process and Figure 1b compares microplasma-treated and untreated colloid samples. The microplasma treated sample remains stable (precipitation-free) for over hundreds of hours post processing. However, precipitation of BN aggregates (indicated by a red arrow in Figure 1b) occurred in the untreated samples 24 h after sonication. The results indicate microplasma processing has significantly improved the dispersion and stability of BNNSs in the solvent.

Figure 2 shows typical transmission electron microscope (TEM) images of microplasma treated and untreated h-BN. The untreated h-BN consists of heavily agglomerated stacked structures (Figure 2a); the width of which ranges from 0.1 to 1 μm (Figure 2a and 2b).While most h-BN sit flat on the TEM grid, the side view of some stacks with multiple BN layers can be observed (in red circles). After the microplasma treatment, the degree of BN nanosheet (BNNS) agglomeration has been

DOI: 10.1021/acsami.6b01531
ACS Appl. Mater. Interfaces 2016, 8, 13567−13572

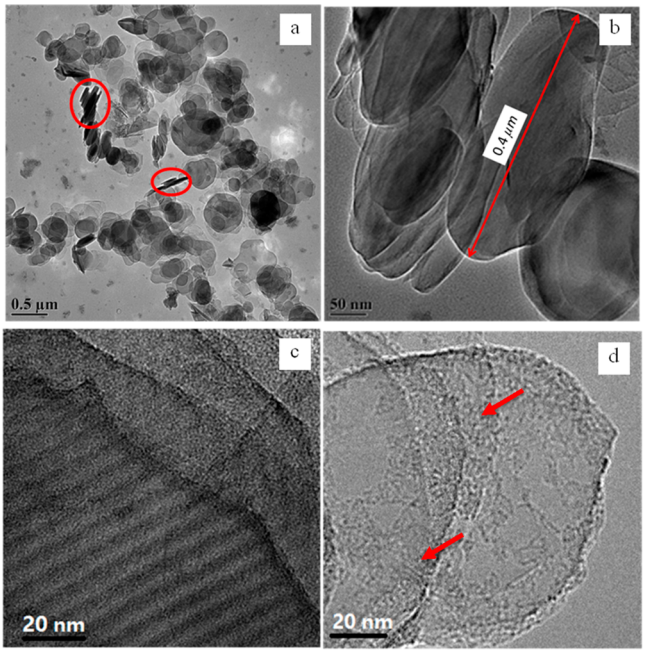

Figure 2. Typical transmission electron microscope images of (a, b, c) untreated and (d) microplasma-treated h-BN (few layers) with amorphous deposit (red arrows).

greatly reduced and few-layer BNNSs can be observed with amorphous surface deposit, Figure 2d.

The microplasma-treated and untreated h-BN were then used to prepare PVA/h-BN nanocomposites to compare their corresponding thermal performance. The PVA/h-BN nanocomposites were obtained by mixing PVA (initially dissolved in 80 °C distilled water) and the plasma treated or untreated h-BN/IPA colloids. The resulting mixtures were heated to 100 °C with vigorous stirring to evaporate the excessive liquid and then the remaining viscous mixtures were spin-coated onto a glass slide to form thin films (~0.5 mm thick). The free-standing PVA/h-BN nanocomposite films were microtomed to form ~100 nm slices for TEM observation.

The in-plane and through-plane thermal diffusivity of the nanocomposite film samples were measured at room temperature. According to Figure 3, the thermal conductivity of the PVA/h-BN nanocomposites (containing plasma treated or untreated h-BN) are highly anisotropic. The in-plane thermal diffusivity is 5−10 times higher than that of the through-plane thermal diffusivity. The sample preparation (spin coating) is expected to induce in-plane orientation of h-BN by the tensile stress applied along the film plane and the compressive stress applied along the film thickness direction during solvent evaporation.[29] Hence the highly anisotropic thermal property is likely to be due to the strong in-plane orientation of the heat-conducting BN basal plane.[30−35]

The thermal diffusivities of nanocomposite films with microplasma-treated or untreated h-BN both increase with increasing h-BN wt % (Figure 3). With 50 wt % h-BN (untreated) in the PVA nanocomposite films, the in-plane thermal diffusivity reaches ~4.6 $mm^2\ s^{-1}$ (Figure 3b), which is ~30 times higher than that of the blank PVA polymer film (0.14 $mm^2\ s^{-1}$). The thermal conductivity (ζ) can be calculated from the thermal diffusivity (α) using eq 1

$$\zeta = dC_p a \quad (1)$$

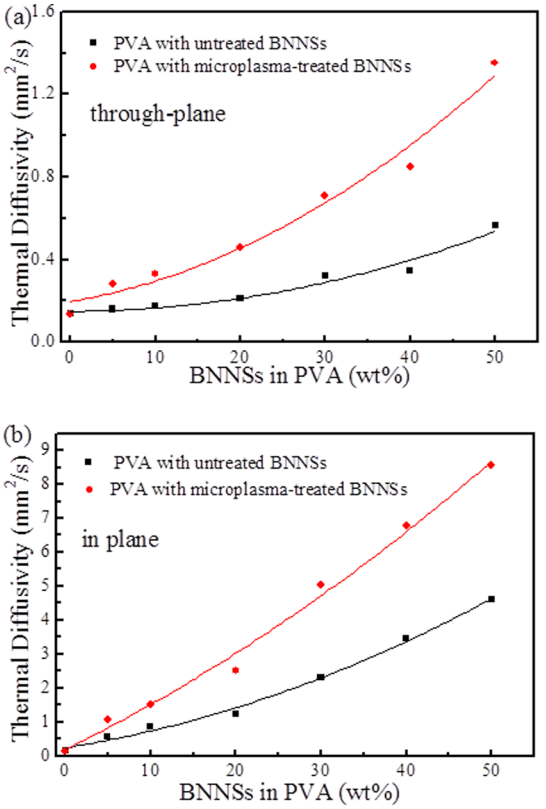

Figure 3. (a) Through-plane and (b) in-plane thermal diffusivities of PVA nanocomposite films with microplasma treated and untreated h-BN at different weight loadings. Measurement accuracy is ±5% from equipment manufacturer's specifications.

where the density (d) and specific heat capacity (C_p) of polymer nanocomposites can be obtained from the corresponding properties of the polymer and the filler using the commonly used rule of mixture[36,37]

$$d_{\text{composite}} = V_{\text{polymer}} \times d_{\text{polymer}} + V_{\text{filler}} \times d_{\text{filler}}$$

It is worth noting that the in-plane thermal diffusivity of PVA nanocomposites with microplasma treated h-BN (50 wt %) is ~8.5 $mm^2\ s^{-1}$ (equivalent to a thermal conductivity of 13 W m K^{-1}), Figure 3b. This is about 50 time higher than blank PVA and double that of nanocomposites containing untreated BNNSs. The thermal diffusivity values of our composites containing plasma treated h-BN is higher than most polymer/BNNSs composites produced by other methods,[16−18,38−44] and is comparable to the highest thermal diffusivity reported for PVA/BN films obtained by mechanical stretching.[6] Furthermore, the trend of the curves shown in Figure 3 suggests that higher thermal diffusivities may be achieved by tuning the BNNSs concentration.

TEM was used to further observe the morphology of h-BN and verify their enhanced dispersion in the PVA matrix, Figure 4. Nanocomposites with untreated h-BN have multilayer stacked BN sheets embedded in the polymer. Figure 4a shows a typical image, where the thickness of untreated h-BN stacked structure is about 10 nm thick. Figure 4b confirms that a typical h-BN stacked structure contains >30 layers. The thickness measurement suggests each individual BN layer within the stack is ~0.33−0.43 nm, consistent with the reported values in the literature.[45,46] Further observation on nanocomposite samples with microplasma-treated h-BN

DOI: 10.1021/acsami.6b01531
ACS Appl. Mater. Interfaces 2016, 8, 13567−13572

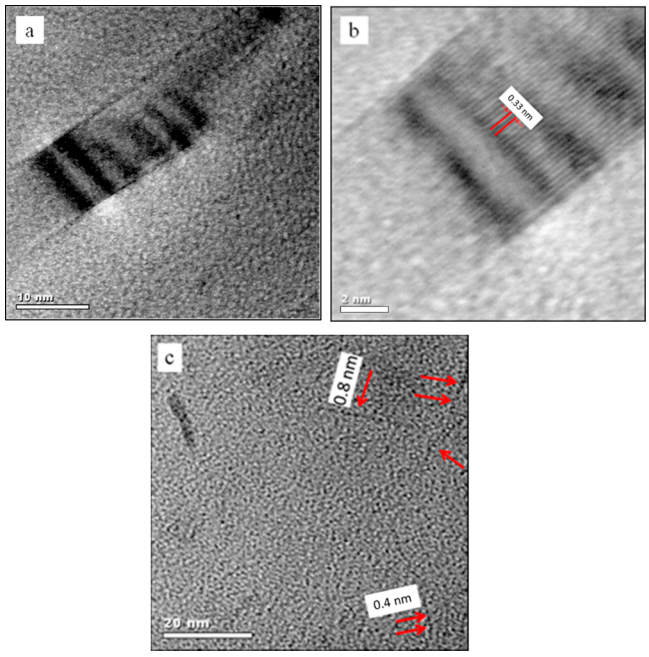

Figure 4. Typical transmission electron microscope images of microtomed PVA nanocomposite films (cross section) containing (a, b) untreated and (c) plasma-treated h-BN.

confirms that heavy aggregates (as those shown in Figure 2a and b) have been greatly reduced. Instead, much thinner BNNSs are formed and these represent the typical features within the PVA matrix. For instance, Figure 4c shows typical plasma treated BNNSs in PVA. Those nanostructures with thickness less than 1 nm indicate formation of single or few-layers nanosheets with a very high aspect ratio (>100).

Generally, heat transfer in polymer nanocomposites occurs through phonons at different frequencies.[47−49] The reduced BN sheet thickness through exfoliation can reduce the interlayer phonon−phonon scattering,[50] hence contributing to a greater heat transport performance. The microplasma-induced exfoliation may be due to the depolarization of B−N bonds caused by the plasma induced highly reactive charged species (e.g., OH^-, solvated electrons), reducing the interlayer bonding force. In addition, the point and line defects present within chemically grown 2D layers would allow the penetration of small ions with the ionic permeability proportional to the size and density of defects.[51]The diameter of defect due to one missing boron atom would be ∼3.11 Å,[52] enough for the penetration of certain reactive species such as OH^- to cause intercalation of BN layers. It is also reported that the accessibility of ions into 2D material is dependent on ion type/size, surface charging and channel width.[53]

On the other hand, the microplasma treatment has induced modification on the h-BN surfaces. As shown in Figure 2d, a dark gray layer of deposit can be seen on the treated BNNS surface. The conversion of IPA into formic acid under plasma discharge has been reported in the literature,[54] where the reaction products is dependent on the energy input and the catalyst presence/properties. Therefore, itis likely new substance such as amorphous carbon containing layer has formed as a result of plasma-IPA interaction, which deposited on the h-BN surface, helping separate the sheets and improve the dispersion and stability of BNNS in the solvent. Figure 5 shows the FITR spectra of microplasma treated and untreated h-BN.

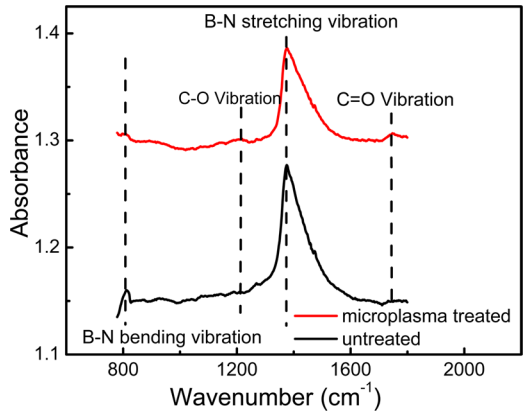

Figure 5. FTIR of h-BN with or without microplasma treatment.

For the microplasma treated sample, new peaks emerge at 1770 and 1210 cm^{-1}. These are similar to those observed in pentanoic acid-functionalized h-BN,[55] and the peaks have been assigned to the C═O stretch and C−O stretch of carboxylic acid.[55]

Within the PVA-BNNS nanocomposites, any gaps or other flaws at the filler−matrix interface arising from insufficient affinity between the inorganic and organic phases would likely enhance the thermal resistance at the interface.[39] Formation of a thin interfacial layer on the BNNS surface may help further improve the thermal interface.[56−58] In our case the carbon-based layer is not uniform across the BNNS surface (Figure 2d), so it may only partially contribute to the improvement of thermal properties. The adsorbed molecules on the surface of BNNS could also physically entangle with the PVA matrix molecules[56] resulting in enhanced interface strength between BNNSs and PVA, leading to the overall improved composite thermal conduction.

CONCLUSIONS

In this work, the use of microplasma processing has demonstrated significant improvement in the thermal performance of nanocomposites comprised of boron nitride nanosheets in PVA. Without plasma treatment BNNS in PVA nanocomposites appear agglomerated and comprised of multilayer stacks whereas after plasma treatment the nanosheets are observed to have been exfoliated with significantly fewer layers and much less agglomeration. Such enhancement of thermal conductivity could be attributed to the improved nanofiller dispersion, better interfacial properties and reduced interlayer phonon scattering. These results demonstrate the advantages of plasma-induced liquid chemistry in the field of nanomaterial synthesis and processing and open the possibilities for additional improvements in nanocomposite materials processing.

METHODS

Materials. h-BN (99%), IPA (99.7%), and PVA (M_w = 85000−124000 and 99% hydrolysis degree) were purchased from Sigma-Aldrich, UK. All the chemical reagents were used as received. The h-BN/IPA mixture was sonicated in low power sonic baths (Branson 1510E-MT) for 24 h to break down the heavy agglomeration [6, 24]. The resultant colloid was centrifuged at 1500 rpm for 30 min, and the supernatant was divided into two samples with equal volume. Samples were subject to further processing via microplasma and compared to reference without plasma treatment.

DOI: 10.1021/acsami.6b01531
ACS Appl. Mater. Interfaces 2016, 8, 13567−13572

Microplasma Processing. the microplasma treatments were carried out with a constant voltage of 3 kV (current varies between 0.1 and 0.9 mA) applied between a stainless steel capillary (0.25 mm inner diameter and 0.5 mm outer diameter) and a carbon counter electrode immersed in the liquid sample being processed (see Figure 1a).The distance between the capillary and the plasma−liquid interface was adjusted to 0.9 mm. The microplasma treatments were carried out for three consecutive 10 min periods, and the mixture is stirred between each period to obtain a well-mixed colloid.

Nanocomposite Films. The PVA powder was dissolved in distilled water (80 °C) and was vigorously stirred for 2 h to produce a PVA aqueous solution (5 mg mL^{-1}). Colloids containing microplasma-treated or untreated BNNSs in IPA were added dropwise to the PVA aqueous solution under constant stirring. The mixtures were concentrated by evaporating the solvents with vigorously stirring (12 h), the remaining liquids were casted on glass slides and films were formed through a spin coating process. The PVA/BNNS nanocomposite films were then dried in a vacuum oven at 100 °C overnight before further analysis. Blank PVA film sample with no BNNS and no plasma treatment was prepared from pure PVA following the same procedures.

Measurements. Transmission electron microscopy (TEM) was performed on a JEOL JEM-2100F. Preparation of cross-sectional microtomed specimen was carried out by first embedding a film sample in epoxy resin, and microtomed into slices with thickness less than 100 nm using a Reichert-Jung Ultracut E. ulstra-Microtome using a 30° angle diamond knife at room temperature. Thermal diffusivity of the PVA/BNNSs nanocomposites was determined using the non-contact laser flash method (LFA-447, Netzsch, Germany) using a xenon flash lamp source at room temperature. The thermal diffusivity was determined by comparing the results with a pyroceramic reference sample. The samples for in-plane thermal diffusivity measurement were about 25.4 mm in diameter, and the samples for through-plane measurements were 12.7 mm × 12.7 mm in size.

AUTHOR INFORMATION

Corresponding Authors

*E-mail: zrcws@zju.edu.cn.

*E-mail: d.sun@qub.ac.uk.

Author Contributions

All authors contributed equally to this work.

Notes

The authors declare no competing financial interest.

ACKNOWLEDGMENTS

This work was financially supported from the National Natural Science Foundation of China (51203135, 51173174) and Invest NI PoC award (no. 325). The authors also wish to acknowledge the support of COST Action TD1208. This work was also partially supported by Engineering & Physical Sciences Research Council (EPSRC) (award n. EP/M024938/1 and EP/K022237/1).

REFERENCES

(1) Alvarez, M. M.; Khoury, J. T.; Schaaff, T. G.; Shafigullin, M. N.; Vezmar, I.; Whetten, R. L. Optical Absorption Spectra of Nanocrystal Gold Molecules. *J. Phys. Chem. B* **1997**, *101*, 3706−3712.

(2) Nahor, O.; Segal-Peretz, T.; Neeman, L.; Oron, D.; Frey, G. L. Controlling Morphology and Charge Transfer in ZnO/Polythiophene Photovoltaic Films. *J. Mater. Chem. C* **2014**, *2*, 4167−4176.

(3) Potts, J. R.; Dreyer, D. R.; Bielawski, C. W.; Ruoff, R. S. Graphene-Based Polymer Nanocomposites. *Polymer* **2011**, *52*, 5−25.

(4) Thanh, N. T. *Magnetic Nanoparticles: From Fabrication to Clinical Applications*; CRC Press, 2012.

(5) Balazs, A. C.; Emrick, T.; Russell, T. P. Nanoparticle Polymer Composites: Where Two Small Worlds Meet. *Science* **2006**, *314*, 1107−1110.

(6) Song, W.-L.; Wang, P.; Cao, L.; Anderson, A.; Meziani, M. J.; Farr, A. J.; Sun, Y.-P. Polymer/Boron Nitride Nanocomposite Materials for Superior Thermal Transport Performance. *Angew. Chem., Int. Ed.* **2012**, *51*, 6498−6501.

(7) Panchal, M. B.; Upadhyay, S. H. Single Walled Boron Nitride Nanotube-Based Biosensor: An Atomistic Finite Element Modelling Approach. *IET Nanobiotechnol.* **2014**, *8*, 149−56.

(8) Kim, G.; Lim, H.; Ma, K. Y.; Jang, A. R.; Ryu, G. H.; Jung, M.; Shin, H.-J.; Lee, Z.; Shin, H. S. Catalytic Conversion of Hexagonal Boron Nitride to Graphene for In-Plane Heterostructures. *Nano Lett.* **2015**, *15*, 4769−4775.

(9) Meyer, N.; Devillers, M.; Hermans, S. Boron Nitride Supported Pd Catalysts for The Hydrogenation of Lactose. *Catal. Today* **2015**, *241*, 200−207.

(10) Lei, W.; Portehault, D.; Liu, D.; Qin, S.; Chen, Y. Porous Boron Nitride Nanosheets for Effective Water Cleaning. *Nat. Commun.* **2013**, *4*, 1777.

(11) Lian, G.; Zhang, X.; Si, H.; Wang, J.; Cui, D.; Wang, Q. Boron Nitride Ultrathin Fibrous Nanonets: One-Step Synthesis and Applications for Ultrafast Adsorption for Water Treatment and Selective Filtration of Nanoparticles. *ACS Appl. Mater. Interfaces* **2013**, *5*, 12773−12778.

(12) Panchal, M. B.; Upadhyay, S. H. Boron Nitride Nanotube-Based Biosensing of Various Bacterium/Viruses: Continuum Modelling-Based Simulation Approach. *IET Nanobiotechnol.* **2014**, *8*, 143−148.

(13) Hu, J.; Ruan, X.; Chen, Y. P. Thermal Conductivity and Thermal Rectification in Graphene Nanoribbons: A Molecular Dynamics Study. *Nano Lett.* **2009**, *9*, 2730−2735.

(14) Ouyang, T.; Chen, Y.; Xie, Y.; Yang, K.; Bao, Z.; Zhong, J. Thermal Transport in Hexagonal Boron Nitride Nanoribbons. *Nanotechnology* **2010**, *21*, 245701.

(15) Lan, J.; Wang, J.-S.; Gan, C. K.; Chin, S. K. Edge Effects on Quantum Thermal Transport in Graphene Nanoribbons: Tight-Binding Calculations. *Phys. Rev. B: Condens. Matter Mater. Phys.* **2009**, *79*, 115401.

(16) Li, T.-L.; Hsu, S. L.-C. Enhanced Thermal Conductivity of Polyimide Films via a Hybrid of Micro- and Nano-Sized Boron Nitride. *J. Phys. Chem. B* **2010**, *114*, 6825−6829.

(17) Sato, K.; Horibe, H.; Shirai, T.; Hotta, Y.; Nakano, H.; Nagai, H.; Mitsuishi, K.; Watari, K. Thermally Conductive Composite Films of Hexagonal Boron Nitride and Polyimide with Affinity-Enhanced Interfaces. *J. Mater. Chem.* **2010**, *20*, 2749−2752.

(18) Li, T.-L.; Hsu, S. L.-C. Preparation and Properties of Thermally Conductive Photosensitive Polyimide/Boron Nitride Nanocomposites. *J. Appl. Polym. Sci.* **2011**, *121*, 916−922.

(19) Golberg, D.; Bando, Y.; Huang, Y.; Terao, T.; Mitome, M.; Tang, C.; Zhi, C. Boron Nitride Nanotubes and Nanosheets. *ACS Nano* **2010**, *4*, 2979−2993.

(20) Jan, R.; May, P.; Bell, A. P.; Habib, A.; Khan, U.; Coleman, J. N. Enhancing The Mechanical Properties of BN Nanosheet-polymer Composites by Uniaxial Drawing. *Nanoscale* **2014**, *6*, 4889−4895.

(21) Meng, W.; Huang, Y.; Fu, Y.; Wang, Z.; Zhi, C. Polymer Composites of Boron Nitride Nanotubes and Nanosheets. *J. Mater. Chem. C* **2014**, *2*, 10049−10061.

(22) Deepika; Li, L. H.; Glushenkov, A. M.; Hait, S. K.; Hodgson, P.; Chen, Y. High-Efficient Production of Boron Nitride Nanosheets via an Optimized Ball Milling Process for Lubrication in Oil. *Sci. Rep.* **2014**, *4*, 7288.

(23) Li, X.; Hao, X.; Zhao, M.; Wu, Y.; Yang, J.; Tian, Y.; Qian, G. Exfoliation of Hexagonal Boron Nitride by Molten Hydroxides. *Adv. Mater.* **2013**, *25*, 2200−2204.

(24) Coleman, J. N.; Lotya, M.; O'Neill, A.; Bergin, S. D.; King, P. J.; Khan, U.; Young, K.; Gaucher, A.; De, S.; Smith, R. J.; Shvets, I. V.; Arora, S. K.; Stanton, G.; Kim, H.-Y.; Lee, K.; Kim, G. T.; Duesberg, G. S.; Hallam, T.; Boland, J. J.; Wang, J. J.; Donegan, J. F.; Grunlan, J. C.; Moriarty, G.; Shmeliov, A.; Nicholls, R. J.; Perkins, J. M.; Grieveson, E. M.; Theuwissen, K.; McComb, D. W.; Nellist, P. D.; Nicolosi, V. Two-Dimensional Nanosheets Produced by Liquid Exfoliation of Layered Materials. *Science* **2011**, *331*, 568−571.

DOI: 10.1021/acsami.6b01531
ACS Appl. Mater. Interfaces 2016, 8, 13567−13572

(25) Liu, Y.; Sun, D.; Askari, S.; Patel, J.; Macias-Montero, M.; Mitra, S.; Zhang, R.; Lin, W.-F.; Mariotti, D.; Maguire, P. Enhanced Dispersion of TiO2 Nanoparticles in a TiO2/PEDOT:PSS Hybrid Nanocomposite via Plasma-Liquid Interactions. *Sci. Rep.* **2015**, *5*, 15765.
(26) Sun, D.; Zhang, R. C.; Wylie, A.; Mira, M. D.; Patel, J.; Manuel-Macias, M.; Askari, S.; Rutherford, D.; Spence, S.; Mariotti, D.; Maguir, P. A Facile Method for Synthesizing PVA/Au, PVA/Ag and PVA/AuAg Nanocomposites. Presented at the 10th International Conference on Composite Science and Technology ICCST/10 Lisbon, 2015.
(27) Mariotti, D.; Švrček, V.; Hamilton, J. W. J.; Schmidt, M.; Kondo, M. Silicon Nanocrystals in Liquid Media: Optical Properties and Surface Stabilization by Microplasma-Induced Non-Equilibrium Liquid Chemistry. *Adv. Funct. Mater.* **2012**, *22*, 954−964.
(28) Sun, D.; Zhang, R. C.; Patel, J.; Askari, S.; Macias-Montero, M.; McDonald, C.; Josheph, P.; Liu, Y.; Mariotti, D.; Maguir, P. A Faile Method for The Synthesis of Au/PEDOT:PSS Nanocomposite. Presented at the 2015 Global Conference on Polymer and Composite Materials (PCM 2015), 2015.
(29) Tanimoto, M.; Yamagata, T.; Miyata, K.; Ando, S. Anisotropic Thermal Diffusivity of Hexagonal Boron Nitride-Filled Polyimide Films: Effects of Filler Particle Size, Aggregation, Orientation, and Polymer Chain Rigidity. *ACS Appl. Mater. Interfaces* **2013**, *5*, 4374−4382.
(30) Veca, L. M.; Meziani, M. J.; Wang, W.; Wang, X.; Lu, F.; Zhang, P.; Lin, Y.; Fee, R.; Connell, J. W.; Sun, Y.-P. Carbon Nanosheets for Polymeric Nanocomposites with High Thermal Conductivity. *Adv. Mater.* **2009**, *21*, 2088−2092.
(31) Balandin, A. A.; Ghosh, S.; Bao, W.; Calizo, I.; Teweldebrhan, D.; Miao, F.; Lau, C. N. Superior Thermal Conductivity of Single-Layer Graphene. *Nano Lett.* **2008**, *8*, 902−907.
(32) Ghosh, S.; Calizo, I.; Teweldebrhan, D.; Pokatilov, E. P.; Nika, D. L.; Balandin, A. A.; Bao, W.; Miao, F.; Lau, C. N. Extremely High Thermal Conductivity of Graphene: Prospects for Thermal Management Applications in Nanoelectronic Circuits. *Appl. Phys. Lett.* **2008**, *92*, 151911.
(33) Peres, N. M. R.; Lopes dos Santos, J. M. B.; Stauber, T. Phenomenological Study of The Electronic Transport Coefficients of Graphene. *Phys. Rev. B: Condens. Matter Mater. Phys.* **2007**, *76*, 073412.
(34) Saito, K.; Nakamura, J.; Natori, A. Ballistic Thermal Conductance of a Graphene Sheet. *Phys. Rev. B: Condens. Matter Mater. Phys.* **2007**, *76*, 115409.
(35) Tian, L.; Anilkumar, P.; Cao, L.; Kong, C. Y.; Meziani, M. J.; Qian, H.; Veca, L. M.; Thorne, T. J.; Tackett, K. N.; Edwards, T.; Sun, Y.-P. Graphene Oxides Dispersing and Hosting Graphene Sheets for Unique Nanocomposite Materials. *ACS Nano* **2011**, *5*, 3052−3058.
(36) Ishida, H.; Rimdusit, S. Heat Capacity Measurement of Boron Nitride-filled Polybenzoxazine: The composite structure-insensitive property. *J. Therm. Anal. Calorim.* **1999**, *58*, 497−507.
(37) Newnham, R. E. *Nonmechanical Properties of Composites: Concise Encyclopedia of Composite Materials*; Kelly, A., Ed.; Pergamon Press: Oxford, U.K., 1994.
(38) Ishida, H.; Rimdusit, S. Very High Thermal Conductivity Obtained by Boron Nitride-filled Polybenzoxazine. *Thermochim. Acta* **1998**, *320*, 177−186.
(39) Xu, Y.; Chung, D. D. L. Increasing The Thermal Conductivity of Boron Nitride and Aluminum Nitride Particle Epoxy-matrix Composites by Particle Surface Treatments. *Compos. Interfaces* **2000**, *7*, 243−256.
(40) Zhou, W.-Y.; Qi, S.-H.; Zhao, H.-Z.; Liu, N.-L. Thermally Conductive Silicone Rubber Reinforced with Boron Nitride Particle. *Polym. Compos.* **2007**, *28*, 23−28.
(41) Wattanakul, K.; Manuspiya, H.; Yanumet, N. Effective Surface Treatments for Enhancing The Thermal Conductivity of BN-filled Epoxy Composite. *J. Appl. Polym. Sci.* **2011**, *119*, 3234−3243.
(42) Kemaloglu, S.; Ozkoc, G.; Aytac, A. Properties of Thermally Conductive Micro and Nano Size Boron Nitride Reinforced Silicon Rubber Composites. *Thermochim. Acta* **2010**, *499*, 40−47.
(43) Morishita, T.; Matsushita, M.; Katagiri, Y.; Fukumori, K. A Novel Morphological Model for Carbon Nanotube/Polymer Composites Having High Thermal Conductivity and Electrical Insulation. *J. Mater. Chem.* **2011**, *21*, 5610−5614.
(44) Yung, K. C.; Liem, H. Enhanced Thermal Cnductivity of Boron Nitride Epoxy-matrix Composite through Multi-modal Particle Size Mixing. *J. Appl. Polym. Sci.* **2007**, *106*, 3587−3591.
(45) Xue, Y.; Liu, Q.; He, G.; Xu, K.; Jiang, L.; Hu, X.; Hu, J. Excellent Electrical Conductivity of the Exfoliated and Fluorinated Hexagonal Boron Nitride Nanosheets. *Nanoscale Res. Lett.* **2013**, *8*, 49.
(46) Li, L. H.; Santos, E. J. G.; Xing, T.; Cappelluti, E.; Roldán, R.; Chen, Y.; Watanabe, K.; Taniguchi, T. Dielectric Screening in Atomically Thin Boron Nitride Nanosheets. *Nano Lett.* **2015**, *15*, 218−223.
(47) Jung, H.; Yu, S.; Bae, N.; Cho, S. M.; Kim, R. H.; Cho, S. H.; Hwang, I.; Jeong, B.; Ryu, J. S.; Hwang, J.; Hong, S. M.; Koo, C. M.; Park, C. High Through-plane Thermal conduction of graphene nanoflake filled polymer composites melt-processed in an L-shape Kinked Tube. *ACS Appl. Mater. Interfaces* **2015**, *7*, 15256−15262.
(48) Yu, S.; Park, I.; Park, C.; Hong, S. M.; Han, T. H.; Koo, C. M. RTA-treated Carbon Fiber/Copper Core/Shell Hybrid for Thermally Conductive Composites. *ACS Appl. Mater. Interfaces* **2014**, *6*, 7498−7503.
(49) Yu, S.; Lee, J. W.; Han, T. H.; Park, C.; Kwon, Y.; Hong, S. M.; Koo, C. M. Copper Shell Networks in Polymer Composites for Efficient Thermal Conduction. *ACS Appl. Mater. Interfaces* **2013**, *5*, 11618−11622.
(50) Lindsay, L.; Broido, D. A. Enhanced Thermal Conductivity and Isotope Effect in Single-layer Hexagonal bBoron Nitride. *Phys. Rev. B: Condens. Matter Mater. Phys.* **2011**, *84*, 155421.
(51) O'Hern, S. C.; Boutilier, M. S. H.; Idrobo, J.-C.; Song, Y.; Kong, J.; Laoui, T.; Atieh, M.; Karnik, R. Selective Ionic Transport through Tunable Subnanometer Pores in Single-Layer Graphene Membranes. *Nano Lett.* **2014**, *14*, 1234−1241.
(52) Jin, C.; Lin, F.; Suenaga, K.; Iijima, S. Fabrication of a Freestanding Boron Nitride Single Layer and Its Defect Assignments. *Phys. Rev. Lett.* **2009**, *102*, 195505.
(53) Bo, Z.; Yang, H.; Zhang, S.; Yang, J.; Yan, J.; Cen, K. Molecular Insights into Aqueous NaCl Electrolytes Confined within Vertically-oriented Graphenes. *Sci. Rep.* **2015**, *5*, 14652.
(54) Rivallan, M.; Fourré, E.; Aiello, S.; Tatibouët, J.-M.; Thibault-Starzyk, F. Insights into The Mechanisms of Isopropanol Conversion on γ-Al2O3 by Dielectric Barrier Discharge. *Plasma Processes Polym.* **2012**, *9*, 850−854.
(55) Sainsbury, T.; Satti, A.; May, P.; O'Neill, A.; Nicolosi, V.; Gun'ko, Y. K.; Coleman, J. N. Covalently Functionalized Hexagonal Boron Nitride Nanosheets by Nitrene Addition. *Chem. - Eur. J.* **2012**, *18*, 10808−10812.
(56) Yu, J.; Mo, H.; Jiang, P. Polymer/boron Nitride Nanosheet Composite with High Thermal Conductivity and Sufficient Dielectric Strength. *Polym. Adv. Technol.* **2015**, *26*, 514−520.
(57) Zhi, C.; Bando, Y.; Tang, C.; Xie, R.; Sekiguchi, T.; Golberg, D. Perfectly Dissolved Boron Nitride Nanotubes Due to Polymer Wrapping. *J. Am. Chem. Soc.* **2005**, *127*, 15996−15997.
(58) Lin, Y.; Williams, T. V.; Connell, J. W. Soluble, Exfoliated Hexagonal Boron Nitride Nanosheets. *J. Phys. Chem. Lett.* **2010**, *1*, 277−283.

DOI: 10.1021/acsami.6b01531
ACS Appl. Mater. Interfaces 2016, 8, 13567−13572